

RESEARCH PAPER

Mitochondrial glycolate oxidation contributes to photorespiration in higher plants

Markus Niessen, Krishnaveni Thiruvedhi, Ruben Rosenkranz, Rashad Kebeish, Heinz-Josef Hirsch, Fritz Kreuzaler and Christoph Peterhänsel*

RWTH Aachen, Institute of Biology I, Worringer Weg 1, D-52056 Aachen, Germany

Received 30 April 2006; Revised 21 May 2007; Accepted 22 May 2007

Abstract

The oxidation of glycolate to glyoxylate is an important reaction step in photorespiration. Land plants and charophycean green algae oxidize glycolate in the peroxisome using oxygen as a co-factor, whereas chlorophycean green algae use a mitochondrial glycolate dehydrogenase (GDH) with organic co-factors. Previous analyses revealed the existence of a GDH in the mitochondria of *Arabidopsis thaliana* (AtGDH). In this study, the contribution of AtGDH to photorespiration was characterized. Both RNA abundance and mitochondrial GDH activity were up-regulated under photorespiratory growth conditions. Labelling experiments indicated that glycolate oxidation in mitochondrial extracts is coupled to CO₂ release. This effect could be enhanced by adding co-factors for aminotransferases, but is inhibited by the addition of glycine. T-DNA insertion lines for AtGDH show a drastic reduction in mitochondrial GDH activity and CO₂ release from glycolate. Furthermore, photorespiration is reduced in these mutant lines compared with the wild type, as revealed by determination of the post-illumination CO₂ burst and the glycine/serine ratio under photorespiratory growth conditions. The data show that mitochondrial glycolate oxidation contributes to photorespiration in higher plants. This indicates the conservation of chlorophycean photorespiration in streptophytes despite the evolution of leaf-type peroxisomes.

Key words: Glycolate dehydrogenase, photorespiration, plant evolution, streptophytes.

Introduction

The land plants (Embryophyta) are a monophyletic group that evolved from green algae. The nearest relatives to extant land plants are found within the charophycean green algae (Karol *et al.*, 2001). Both lineages are often subsumed under the term streptophytes based on both cytological and molecular evidence (Lewis and McCourt, 2004). One important feature shared by streptophytes is the presence of leaf-type peroxisomes containing glycolate oxidase (GO) as a key enzyme (Igamberdiev and Lea, 2002). The substrate glycolate is produced in plant and algal chloroplasts from phosphoglycolate, that is itself a primary product of the oxygenase activity of ribulose-1,5-bisphosphate carboxylase/oxygenase (Rubisco). This activity is a seemingly inevitable but important side reaction of carbon fixation by Rubisco and makes up approximately one-quarter of all Rubisco catalytic events under standard conditions in most higher plants (Sharkey, 2001). The complete process of recycling the products of the oxygenase activity of Rubisco is referred to as photorespiration (Stabenau and Winkler, 2005; Reumann and Weber, 2006). Streptophytes oxidize glycolate to glyoxylate catalysed by GO in the peroxisomes and concomitantly reduce molecular oxygen to hydrogen peroxide. Glyoxylate is transaminated to glycine in the peroxisome and exported to mitochondria where two molecules of glycine react to form one molecule of serine with the release of CO₂ and NH₃. Serine is transported back to the peroxisome where it is converted to hydroxypyruvate and further reduced to glycerate. Finally, glycerate is transported to the chloroplast and phosphorylated to phosphoglycerate that can be re-integrated into the Calvin cycle. By this sequence of reactions, three-quarters of the carbon from phosphoglycolate can be salvaged.

In contrast, leaf-type peroxisomes are absent in chlorophytes, the second large lineage of green algae, that subsumes the classes Chlorophyceae, Ulvophyceae, and Trebouxiophyceae (Frederick *et al.*, 1973). Besides simply secreting glycolate from the cell, this group uses a mitochondrial glycolate dehydrogenase (GDH) for the production of glyoxylate that most probably transfers electrons to the respiratory electron chain (Paul and Volcani, 1976). Recent analyses in the trebouxiophycean species *Eremosphaera viridis* revealed that the subsequent metabolism is similar to photorespiration in streptophytes but that all reactions are located in mitochondria and the capacity of this pathway to convert glycolate is lower compared with the streptophyte pathway (Stabenau and Winkler, 2005). However, the importance of the mitochondrial GDH in chlorophytes has been demonstrated by the characterization of a *Chlamydomonas* strain carrying a plasmid insertion in the corresponding gene. The mutation is conditionally lethal and the strain is only capable of growing at elevated CO₂ concentrations where the oxygenase activity of Rubisco is low (Nakamura *et al.*, 2005). This is reminiscent of photorespiratory mutants in higher plants (Somerville and Ogren, 1982).

The clear differentiation of glycolate metabolism in streptophytes and chlorophytes was recently questioned due to the identification of a GDH targeted to the mitochondria of the higher land plant *Arabidopsis thaliana* (*AtGDH*) (Bari *et al.*, 2004). In this report, evidence is provided that *AtGDH* contributes to glycolate metabolism in *Arabidopsis*, indicating conservation of the chlorophyte pathway in higher plants.

Materials and methods

Plant growth

Plants used for physiological experiments were grown under short-day conditions (8 h illumination and 16 h darkness) in growth chambers at 22 °C with a light intensity of 100 μmol m⁻² s⁻¹. For low CO₂ treatments, the plants were shifted to a growth cabinet that was constantly supplied with air containing 100 ppm CO₂.

The *AtGDH* T-DNA insertion mutants were ordered from the Nottingham Arabidopsis Stock Centre (NASC). Homozygous mutants were identified by PCR using the primers and conditions as suggested by NASC.

Real-time RT-PCR

RNA was prepared from *Arabidopsis* leaves following the BCP (1-bromo-3-chloropropane) protocol (Chomczynski and Mackey, 1995). The integrity of the preparation was tested by gel electrophoresis.

One unit of DNase I (Roche Applied Science) per microgram of RNA and MgCl₂ to a final concentration of 2 mM were added and the reactions were incubated for 15 min at 37 °C, followed by a denaturation step of 15 min at 70 °C to remove traces of contaminating DNA.

Approximately 1 μg of RNA was mixed with 10 pmol oligo(dT) primer, heated for 5 min to 70 °C and cooled down on ice before adding 200 U of Moloney murine leukaemia virus reverse transcriptase (Promega) and 1 mM dNTPs in reaction buffer supplied

by the manufacturer. Quantitative PCRs were performed on an ABI PRISM[®] 7000 Sequence Detection System (Applied Biosystems) following the manufacturer's instructions. Amplifications were performed in the presence of SYBR Green (qPCR core kit for SYBR Green I; Eurogentec) as the fluorescent dye. Reaction kits were derived from Eurogentec, and oligonucleotides were purchased from Metabion. For the detection of *AtGDH* transcripts, primers were 5'-CCTTGCAGAACTCATATCAAGATC-3' and 5'-CATGAGGAGGAAGAATTAACCTTTCC-3' with a final primer concentration of 300 nM in the reaction mixture. For the detection of *Actin2* transcripts, primers were 5'-GGTAACATTGTGCT-CAGTGGTGG-3' and 5'-GGTGAACGACCTTAATCTTCAT-3' with a final primer concentration of 900 nM in the reaction mixture. The MgCl₂ concentration was always 2 mM and the dNTP concentration 200 μM. Amplification conditions were 10 min of initial denaturation at 95 °C, followed by 40 cycles each of 15 s denaturation at 95 °C and 1 min combined annealing and extension at 60 °C.

Mitochondria isolation and enzymatic assays

Intact mitochondria were isolated from 4-week-old *Arabidopsis* plants. Approximately 5 g of leaf material was ground in 200 ml of grinding buffer [50 mM HEPES-KOH pH 7.5, 1 mM MgCl₂, 1 mM EDTA, 1 g l⁻¹ bovine serum albumin (BSA), 0.2 g l⁻¹ sodium ascorbate, 0.3 M mannitol, 5 g l⁻¹ polyvinyl pyrrolidone (PVP)]. After filtration through three layers of Miracloth, the solution was centrifuged at 1100 g for 20 min. The supernatant was centrifuged again at 14 000 g for 30 min. The pellets were resuspended in mannitol wash buffer (10 mM HEPES-KOH pH 7.5, 0.3 M mannitol and 1 g l⁻¹ BSA), and this solution was loaded on a self-forming 8 ml 45% Percoll gradient [45% Percoll, 50% sucrose buffer (0.3 M sucrose, 10 mM HEPES-KOH pH 7.5 and 1 g l⁻¹ BSA)]. The gradient was centrifuged for 45 min at 40 000 g. The mitochondrial fraction was collected and washed in mannitol wash buffer. The mitochondrial protein was extracted in extraction buffer (50 mM HEPES-NaOH pH 7.5, 2 mM EDTA, 5 mM MgCl₂, 0.1% Triton X-100 and 30% glycerol). The absence of peroxisomes in the preparation was determined by the catalase activity assay. For this, the protein solution was adjusted to 30 mM phosphate buffer pH 7.0 and 10 mM H₂O₂, and the enzymatic activity was measured at 240 nm wavelength. The measured purity was always higher than 95%.

GDH activity was assayed according to Lord (1972). Protein extract containing 100 μg of protein was added to 10 mM potassium phosphate (pH 8.0), 0.025 mM DCIP, 0.1 ml of 1% (w/v) PMS, and 10 mM potassium glycolate. At fixed time points, individual assays were terminated by the addition of 0.1 ml of 12 M HCl. After incubation for 10 min, 0.5 ml of 0.1 M phenylhydrazine-HCl was added. The mixture was allowed to incubate again for 10 min. Then the extinction due to the formation of glyoxylate phenylhydrazone was measured at 324 nm.

CO₂ release from labelled substrates in mitochondrial extracts

[1,2-¹⁴C]Glycolate or [1-¹⁴C]glycine (37 kBq) (Hartmann Analytisch, Braunschweig, Germany) was added to 50–100 μg of mitochondrial protein extract in a tightly closed 15 ml reaction tube. Specific radioactivities are 1850 MBq mmol⁻¹ for [1,2-¹⁴C]glycolate and 2109 MBq mmol⁻¹ for [1-¹⁴C]glycine. Final concentrations in the reaction mix are 0.1 mM [1,2-¹⁴C]glycolate and 0.09 mM [1-¹⁴C]glycine. Released CO₂ was absorbed in a 500 μl reaction tube containing 0.5 M NaOH attached to the inner wall of the 15 ml tube. Samples were incubated for 5 h and the gas phase in the reaction tube was mixed frequently with a syringe.

For inhibition experiments, non-labelled glycine was added in different concentrations to the assay mix. The dependence on transamination was measured by adding 0.5 mM pyridoxal-5-phosphate, 0.5 mM MgCl₂, and 1 mM alanine or glutamate, respectively.

Determination of glycine and serine

For the determination of glycine and serine, whole leaf rosettes were harvested and immediately frozen in liquid nitrogen. The abundance of the amino acids was analysed and quantified by gas chromatography-mass spectrometry (GC-MS) using a Chemstation 5890 Series II gas chromatograph (Hewlett Packard). Extraction and derivatization of samples were performed as described by Wagner *et al.* (2003). A dilution series of standard substances for peak identification was prepared and a SIM-mode was implemented for quantification of each substance. The *m/z* values were: glycine (147, 174, 248); serine (116, 204, 218); and ribitol (205, 217, 319). Peak areas were integrated by the auto-integration software supplied by the manufacturer.

Gas exchange measurements

Gas exchange measurements were performed using the LI-6400 system (Li-Cor, Lincoln, NE, USA) and parameters were calculated with the software supplied by the manufacturer. Conditions were: photon flux density (PPFD), 1000 $\mu\text{mol m}^{-2} \text{s}^{-1}$; chamber temperature, 26 °C; flow rate, 100 $\mu\text{mol s}^{-1}$; *c*_a, 100 ppm, relative humidity, 60–70%. The post-illumination CO₂ burst (PIB) was measured as described earlier (Atkin *et al.*, 1998). In brief, plants were incubated under photorespiratory conditions and shifted to the dark. CO₂ fixation stops earlier than photorespiration under these conditions. This results in a transient peak in the CO₂ release curve before the steady-state rates of dark respiration (*R*_n) are reached. The height of this peak correlates with the amount of CO₂ released in photorespiration. The assimilation rates were recorded continuously every 2 s throughout the measurement.

Statistical analysis

Significance was determined according to the *t*-test using Excel software (Microsoft, Munich, Germany). Two-sided tests were performed for homoscedastic matrices.

Results

Induction of AtGDH RNA accumulation and activity under photorespiratory conditions

AtGDH is expressed in leaves, flowers, stems, and roots, but shows preferential RNA accumulation in illuminated green leaves (Bari *et al.*, 2004). In order to test whether the corresponding gene is induced by photorespiratory conditions, wild-type plants were shifted from ambient atmosphere (400 ppm CO₂) to 100 ppm CO₂ for 28 h. The low CO₂ treatment induced the accumulation of AtGDH RNA by a factor of 2.5 (Fig. 1A). Mitochondria were also isolated from these plants and the enzymatic activity of AtGDH was measured. The mitochondrial preparations were free from contamination by peroxisomes according to measurements of catalase activity (310 ± 31 $\mu\text{mol } \mu\text{g}^{-1} \text{min}^{-1}$ for the crude extract and 4 ± 3 $\mu\text{mol } \mu\text{g}^{-1} \text{min}^{-1}$ for the mitochondrial extract). Appreciable GDH activity was measured at 400 ppm that

was again induced by a factor of 2.5 under low CO₂ conditions (Fig. 1B). This activity could be completely inhibited by addition of KCN, a typical property of GDH enzymes, but not of GO enzymes (data not shown). The data indicate that AtGDH activity is induced by photorespiratory conditions at the transcriptional level.

Identification of AtGDH T-DNA insertion lines

Two putative T-DNA insertion lines for AtGDH were identified in the databases of the NASC European Arabidopsis Stock Centre. Line N501490 (N50) carries a T-DNA insertion in the second last exon of the AtGDH coding sequence, whereas the insertion is found in intron 5 in line N526859 (N52). Segregants homozygous for the T-DNA integration were identified by PCR. Neither mutant showed any obvious phenotypic deviation from the wild type under standard growth conditions. In both lines, AtGDH RNA amounts were reduced by a factor of >20 and at the detection limit of the reverse transcription-PCR (RT-PCR) (Fig. 2A). Concomitantly, a similar decrease in AtGDH activity of mitochondrial extracts from line N52 could be found (Fig. 2B). It was concluded that the AtGDH gene has been efficiently disrupted in the mutant lines. Furthermore, assay results from these lines provide independent evidence that the activity assay is specific for AtGDH and not influenced by contaminating peroxisomal GO activity.

Glycolate metabolism in isolated mitochondria

In order to understand whether mitochondrial glycolate oxidation is coupled to photorespiratory CO₂ release, extracts from isolated mitochondria were incubated with [¹⁴C]glycolate, and radioactive CO₂ released from the reaction mixture was absorbed in NaOH. AtGDH mutants showed a drastic decrease in CO₂ release from glycolate compared with the wild type (Fig. 3A). However, CO₂ release from glycine was similar for wild-type and mutant extracts (Fig. 3B). The rate of CO₂ release from glycine in wild-type extracts was ~30-fold higher compared with the release from glycolate. Importantly, CO₂ release from glycolate could be inhibited by the addition of excess unlabelled glycine (Fig. 3C). The data indicate that glyoxylate produced in the mitochondria is further metabolized in a reaction pathway that involves the decarboxylation of glycine. The conversion of glyoxylate to glycine might be catalysed by aminotransferases, and putative alanine:glyoxylate aminotransferases were localized to mitochondria by both bioinformatic prediction [At2g38400, At1g72330, and At1g17290 according to PSORT (Nakai and Horton, 1999)] and organelle proteome analyses (Millar *et al.*, 2001; Ito *et al.*, 2006). An experiment was therefore conducted to test whether addition of an amino donor would increase mitochondrial CO₂ release from labelled glycolate. As shown in Fig. 3D, addition of 50 mM alanine enhanced CO₂ release by a factor of seven. However, this effect was

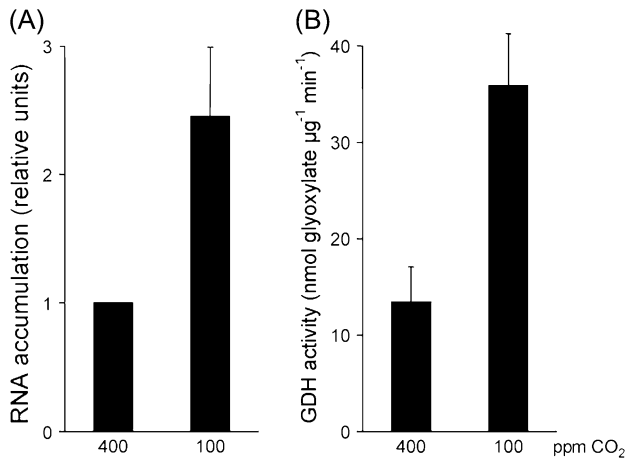


Fig. 1. Induction of *AtGDH* RNA accumulation and protein activity under photorespiratory conditions. Plants were grown under standard growth conditions (400 ppm CO₂) or shifted for 28 h to 100 ppm CO₂. Each data point represents three (RNA) or four (activity) independent experiments. Error bars indicate the SEM. (A) *AtGDH* mRNA abundance standardized for the abundance of the *Actin2* transcript. Values measured at 400 ppm are set as 1. (B) GDH activity from isolated mitochondrial protein.

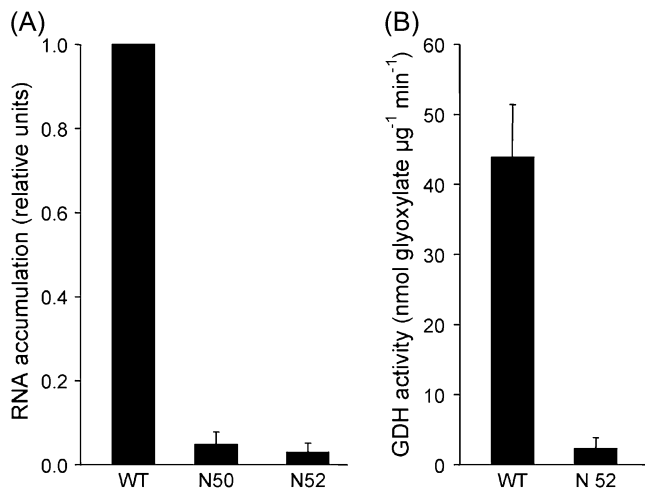


Fig. 2. Reduction of RNA accumulation and protein activity in *AtGDH* mutants. Each data point is based on at least three independent experiments. Error bars indicate the SEM. WT, wild type; N50, NASC T-DNA insertion mutant N501490; N52, NASC T-DNA insertion mutant N526859. (A) *AtGDH* mRNA abundance in wild-type and mutant lines standardized for the abundance of the *Actin2* transcript. Results for the wild type are set as 1. (B) GDH activity in mitochondrial extracts isolated from wild-type and mutant plants.

clearly attenuated ($P=0.003$) when the same amount of glutamate was used. This suggests that alanine acts as the amino donor for the transamination of glyoxylate in mitochondria.

Reduced metabolite flow through photorespiration in *AtGDH* mutants

Two techniques were used to measure the rate of photorespiration in *AtGDH* mutants. First, the PIB was

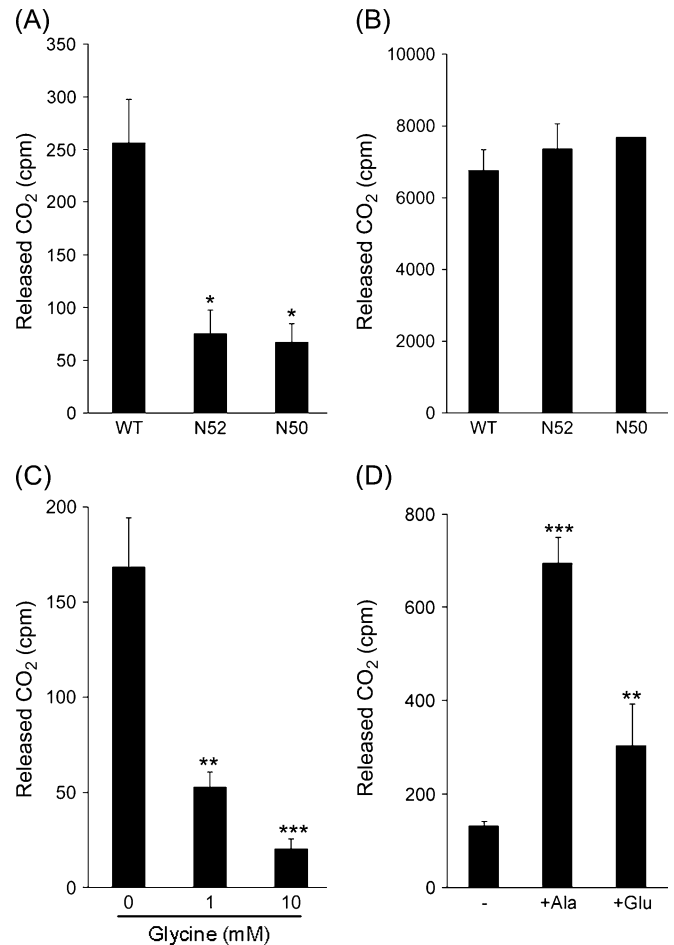


Fig. 3. CO₂ release from isolated mitochondrial extracts. ¹⁴C-Labelled substrates were added to protein extracts of isolated mitochondria and the evolving CO₂ was captured in an NaOH trap. cpm, Counts per minute per μg of mitochondrial protein; WT, wild type; N50, NASC T-DNA insertion mutant N501490; N52, NASC T-DNA insertion mutant N526859. Each data point represents at least three independent experiments. Error bars indicate the SEM. * $P < 0.05$, ** $P < 0.01$, *** $P < 0.001$. (A) CO₂ release from glycolate (0.1 mM, 37 kBq) in mitochondrial extracts from wild-type and mutant lines. (B) CO₂ release from glycine (0.09 mM, 37 kBq) in mitochondrial extracts from wild-type and mutant lines. (C) Inhibition of CO₂ release from glycolate (0.1 mM, 37 kBq) by different concentrations (1 mM and 10 mM) of non-labelled glycine in wild-type mitochondrial extracts. (D) CO₂ release from glycolate (0.1 mM, 37 kBq) in wild-type mitochondrial extracts after addition of 1 mM alanine (Ala) or glutamate (Glu).

determined as a quantitative indicator for CO₂ release from the mitochondrial glycine decarboxylase reaction (Laisk and Sumberg, 1994). As shown in Fig. 4, both mutant lines showed a significant reduction in photorespiratory CO₂ release compared with the wild type. Secondly, the ratio of the abundance of glycine and serine in leaves (Gly/Ser ratio) was determined. This parameter shows a good correlation with the rate of photorespiration (Novitskaya *et al.*, 2002). Accordingly, the Gly/Ser ratio strongly increased in wild-type plants from values of around 1 to >20 when plants were shifted from ambient conditions to 100 ppm CO₂. The mutant lines N50

and N52 showed similar Gly/Ser ratios to the wild type under ambient conditions, but the increase under photorespiratory conditions was clearly weaker. The results suggest that mitochondrial glycolate oxidation contributes to photorespiration in *Arabidopsis*.

Discussion

The main photorespiratory pathway in higher plants (see Introduction) has been well defined by both biochemical and genetic studies (Tolbert, 1997). Mutants in most genes encoding enzymes involved in this pathway have been shown to be incapable of growing at atmospheric CO₂ concentrations (Somerville and Ogren, 1982), indicating the importance of this pathway for the metabolism of glycolate. In contrast, the *AtGDH* mutants identified in this study show a phenotype indistinguishable from the wild type under standard growth conditions. Mitochondrial glycolate oxidation is therefore seemingly not essential for photorespiration. However, higher plant photorespiration shows significant plasticity and uses additional biochemical pathways in addition to the main pathway. For instance, chloroplast extracts are capable of oxidizing glycolate (Goyal and Tolbert, 1996; Kebeish *et al.*, 2007) and glyoxylate (Kisaki and Tolbert, 1969; Oliver, 1981; Zelitch, 1972) to CO₂ without the involvement of peroxisomes or mitochondria. A second example is the non-enzymatic decarboxylation of glyoxylate to formate in the peroxisome. The resulting C1-compound can serve as a carbon donor in the mitochondrial synthesis of serine from glycine (Singh *et al.*, 1986; Wingler *et al.*, 1999, 2000). This pathway does not involve transamination reactions and is therefore suggested to be important under conditions of low nitrogen supply. Analogously, mitochondrial glycolate oxidation might contribute to photorespiration under conditions where the peroxisomal pathway is not sufficient to metabolize all of the glycolate coming from the oxygenase activity of Rubisco. The function as a valve for excess glycolate is in accordance with the significant reduction of both the PIB and the Glyc/Ser ratio (Figs 4, 5) in *AtGDH* mutants. Both parameters are measured under conditions of high oxygenase activity, and *AtGDH* transcription and activity are induced under such conditions (Fig. 1). In contrast, the capacity of mitochondrial extracts from plants grown under standard conditions to oxidize glycolate is 10% or less of the capacity to oxidize glycine (Fig. 3). Mitochondrial glycolate oxidation is seemingly occurring, but dispensable under these conditions. This is supported by the fact that knock-outs and overexpressing lines for the genes encoding any of the potentially mitochondrial alanine:glyoxylate aminotransferases (mAGATs) also show no obvious phenotype (N Stabler, S Gartner, M Niessen, C Peterhansel, unpublished data).

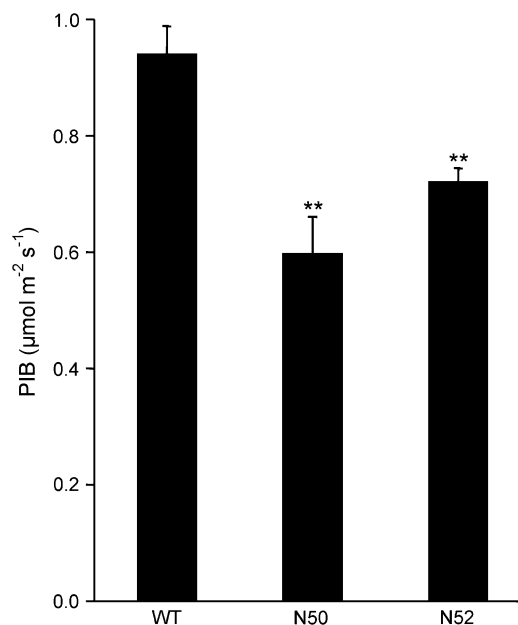


Fig. 4. Reduction of the post-illumination CO₂ burst (PIB) in *AtGDH* mutant lines. Quantification of the PIB. WT, wild type; N50, NASC T-DNA insertion mutant N501490; N52, NASC T-DNA insertion mutant N526859. Plants were adapted to 100 ppm CO₂ and 1000 μmol m⁻² s⁻¹ light before the measurement. Photosynthetic rates at the start of the measurement were ~1 μmol m⁻² s⁻¹. Each data point represents measurements from at least five independent plants. Error bars indicate the SEM. ***P* < 0.01.

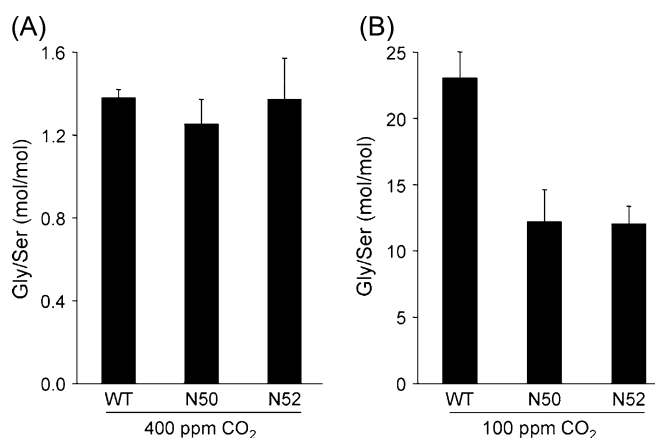


Fig. 5. Reduction of photorespiration in *AtGDH* mutant lines. Ratio of the molar abundance of glycine and serine in plants grown at (A) 400 ppm CO₂ or (B) shifted to 100 ppm CO₂ for 28 h. WT, wild type; N50, NASC T-DNA insertion mutant N501490; N52, NASC T-DNA insertion mutant N526859. Each data point represents at least three independent plants. Error bars indicate the SEM. *P*-values for deviations from the wild type at 100 ppm CO₂ are 0.12 (N50) and 0.06 (N52).

It is assumed that glyoxylate produced by *AtGDH* is transaminated to glycine and afterwards decarboxylated by the mitochondrial glycine decarboxylase complex. First, bioinformatic and proteomic analyses support the existence of one or more mAGAT enzymes (see Results). Secondly, glycolate metabolism in mitochondrial extracts is coupled to CO₂ release and this can be almost

completely inhibited by the addition of unlabelled glycine, but enhanced by the addition of alanine (Fig. 3). Thirdly, this effect is attenuated when glutamate is added instead of alanine, an enzymatic property that separates the mitochondrial enzyme from the peroxisomal glutamate:glyoxylate aminotransferase (GGAT) and that accepts alanine and glutamate as amino donors with similar efficiency (Nakamura and Tolbert, 1983). Previous analyses in oat suggested that amino groups from alanine fed to leaf discs are integrated into glycine with even higher efficiency compared with glutamate (Betsche, 1983), a fact that cannot be explained by the enzymatic properties of GGAT, but that might be brought about in part by mAGAT enzymes.

Peroxisomal and mitochondrial glycolate metabolism share the same reaction steps: oxidation of glycolate followed by transamination to glycine. It is therefore feasible to assume that the pathways are partially redundant and can complement each other. In this context, it is interesting that mutants in the peroxisomal oxidase (GO) and GGAT have never been isolated in direct screens for photorespiratory mutants, whereas the other genes of the photorespiratory cycle were tagged in conditional mutants that survive at high CO₂ but are not viable at ambient CO₂ concentrations (Wingler *et al.*, 2000; Reumann and Weber, 2006). Moreover, a drastic reduction of GO levels in tobacco by RNA co-suppression resulted in a light-sensitive phenotype, but these plants did not require high CO₂ for normal growth when the light intensity was reduced (Yamaguchi and Nishimura, 2000). Similarly, a T-DNA integration in the gene encoding the vast amount of peroxisomal GGAT in *Arabidopsis* reduced but did not abolish growth at ambient CO₂ (Igarashi *et al.*, 2003). These data might be interpreted to indicate that genes are partially redundant (Igarashi *et al.*, 2003) or that homozygous mutations are embryo-lethal. It is alternatively suggested that the capacity of mitochondrial glycolate oxidation is sufficient to rescue such mutants and to allow conversion of most of the phosphoglycolate synthesized by the oxygenase activity of Rubisco at ambient growth conditions.

Higher plant mitochondrial glycolate oxidation has been described so far exclusively in *Arabidopsis* (Bari *et al.*, 2004). It therefore cannot be excluded that this is a peculiarity of this species. The nearest homologue in the rice transcriptome is sequence AK067700 in GenBank, but prediction of translation products indicates early stop codons. Removal of a potential intron sequence and shifting of a splice acceptor site to an alternative site by 7 bp results in a coding sequence that shows very high homology to AtGDH (80% identity and 91% similarity on the amino acid level; M Niessen, C Peterhänsel, unpublished results). Thirty-one rice expressed sequence tags (ESTs) with >95% identity to the 3' end of this sequence according to MegaBLAST argue for the exis-

tence of this assembled RNA (Altschul *et al.*, 1997). However, it remains to be shown whether rice mitochondria also contain the corresponding activity.

In this work, evidence is provided that mitochondrial and peroxisomal glycolate metabolism co-exist in *Arabidopsis*. Previous analyses indicated that charophycean green algae, the nearest relatives to land plants, shifted glycolate oxidation from the mitochondrion to the peroxisome (Stabenau and Winkler, 2005). However, the mitochondrial and the peroxisomal enzyme show no homology on the protein level and differ in important enzymatic properties (Bari *et al.*, 2004). The protein was therefore not simply re-targeted. It remains elusive why GDH activity cannot be detected in charophytes (Stabenau and Winkler, 2005) but in at least one higher plant. One reasonable explanation is that the common ancestor of charophytes and higher plants still contained both enzymes, and mitochondrial GDH was lost secondarily during charophyte evolution. A survey of glycolate-oxidizing enzymes in algae revealed that peroxisomal glycolate oxidation evolved polyphyletically (Suzuki *et al.*, 1991; Igamberdiev and Lea, 2002). Besides charophytes, red algae (Rhodophyta) mainly contain peroxisomes with GO, whereas in diatoms two GDHs in mitochondria and peroxisomes co-exist that both use organic co-factors. The main advantage of mitochondrial glycolate oxidation seems to be the direct coupling to the electron transport chain that allows the recovery of energy equivalents, whereas the peroxisomal enzyme reactions have much higher specific activities (Paul and Volcani, 1976; Stabenau and Winkler, 2005). A combination of both pathways in a single cell might provide the plant with an optimized adaptability to changes in environmental conditions.

Acknowledgements

The authors are grateful to Ina Horst and Yvonne Phlippen for critical reading of the manuscript, and to Burkhard Schmidt for help with GC analyses.

References

- Altschul SF, Madden TL, Schaffer AA, Zhang J, Zhang Z, Miller W, Lipman DJ. 1997. Gapped BLAST and PSI-BLAST: a new generation of protein database search programs. *Nucleic Acids Research* **25**, 3389–3402.
- Atkin OK, Evans JR, Siebke K. 1998. Relationship between the inhibition of leaf respiration by light and enhancement of leaf dark respiration following light treatment. *Australian Journal of Plant Physiology* **25**, 437–443.
- Bari R, Kebeish R, Kalamajka R, Rademacher T, Peterhänsel C. 2004. A glycolate dehydrogenase in the mitochondria of *Arabidopsis thaliana*. *Journal of Experimental Botany* **55**, 623–630.
- Betsche T. 1983. Aminotransfer from alanine and glutamate to glycine and serine during photorespiration in oat leaves. *Plant Physiology* **71**, 961–965.

- Chomczynski P, Mackey K.** 1995. Substitution of chloroform by bromo-chloropropane in the single-step method of RNA isolation. *Analytical Biochemistry* **225**, 163–164.
- Frederick SE, Gruber PJ, Tolbert NE.** 1973. The occurrence of glycolate dehydrogenase and glycolate oxidase in green plants: an evolutionary survey. *Plant Physiology* **52**, 318–323.
- Goyal A, Tolbert NE.** 1996. Association of glycolate oxidation with photosynthetic electron transport in plant and algal chloroplasts. *Proceedings of the National Academy of Sciences, USA* **93**, 3319–3324.
- Igamberdiev AU, Lea PJ.** 2002. The role of peroxisomes in the integration of metabolism and evolutionary diversity of photosynthetic organisms. *Phytochemistry* **60**, 651–674.
- Igarashi D, Miwa T, Seki M, Kobayashi M, Kato T, Tabata S, Shinozaki K, Ohsumi C.** 2003. Identification of photorespiratory glutamate:glyoxylate aminotransferase (GGAT) gene in *Arabidopsis*. *The Plant Journal* **33**, 975–987.
- Ito J, Heazlewood JL, Millar AH.** 2006. Analysis of the soluble ATP-binding proteome of plant mitochondria identifies new proteins and nucleotide triphosphate interactions within the matrix. *Journal of Proteome Research* **5**, 3459–3469.
- Karol KG, McCourt RM, Cimino MT, Delwiche CF.** 2001. The closest living relatives of land plants. *Science* **294**, 2351–2353.
- Kebeish R, Niessen M, Thiruveedhi K, Bari R, Hirsch H-J, Rosenkranz R, Stähler N, Schönfeld B, Kreuzaler F, Peterhänsel C.** 2007. Chloroplastic photorespiratory bypass increases photosynthesis and biomass production in *Arabidopsis thaliana*. *Nature Biotechnology* **25**, 593–599.
- Kisaki T, Tolbert NE.** 1969. Glycolate and glyoxylate metabolism by isolated peroxisomes or chloroplasts. *Plant Physiology* **44**, 242–250.
- Laisk A, Sumberg A.** 1994. Partitioning of the leaf CO₂ exchange into components using CO₂ exchange and fluorescence measurements. *Plant Physiology* **106**, 689–695.
- Lewis LA, McCourt RM.** 2004. Green algae and the origin of land plants. *American Journal of Botany* **91**, 1535–1556.
- Lord JM.** 1972. Glycolate oxidoreductase in *Escherichia coli*. *Biochimica et Biophysica Acta* **267**, 227–237.
- Millar AH, Sweetlove LJ, Giege P, Leaver CJ.** 2001. Analysis of the *Arabidopsis* mitochondrial proteome. *Plant Physiology* **127**, 1711–1727.
- Nakai K, Horton P.** 1999. PSORT: a program for detecting sorting signals in proteins and predicting their subcellular localization. *Trends in Biochemical Sciences* **24**, 34–35.
- Nakamura Y, Kanakagiri S, Van K, He W, Spalding M.** 2005. Disruption of the glycolate dehydrogenase gene in the high-CO₂-requiring mutant HCR89 of *Chlamydomonas reinhardtii*. *Canadian Journal of Botany* **83**, 820–833.
- Nakamura Y, Tolbert NE.** 1983. Serine:glyoxylate, alanine:glyoxylate, and glutamate:glyoxylate aminotransferase reactions in peroxisomes from spinach leaves. *Journal of Biological Chemistry* **258**, 7631–7638.
- Novitskaya L, Trevanion SJ, Driscoll S, Foyer CH, Noctor G.** 2002. How does photorespiration modulate leaf amino acid contents? A dual approach through modelling and metabolite analysis. *Plant, Cell and Environment* **25**, 821–835.
- Oliver DJ.** 1981. Role of glycine and glyoxylate decarboxylation in photorespiratory CO₂ release. *Plant Physiology* **68**, 1031–1034.
- Paul JS, Volcani BE.** 1976. A mitochondrial glycolate:cytochrome *c* reductase in *Chlamydomonas reinhardtii*. *Planta* **129**, 59–61.
- Reumann S, Weber APM.** 2006. Plant peroxisomes respire in the light: some gaps of the photorespiratory C₂ cycle have become filled—others remain. *Biochimica et Biophysica Acta* **1763**, 1496.
- Sharkey TD.** 2001. Photorespiration. *Encyclopedia of Life Sciences* 1–5.
- Singh P, Kumar PA, Abrol YP, Naik MS.** 1986. Photorespiratory nitrogen cycle—a critical evaluation. *Physiologia Plantarum* **66**, 169–176.
- Somerville CR, Ogren WL.** 1982. Genetic modification of photorespiration. *Trends in Biochemical Sciences* **7**, 171–174.
- Stabenau H, Winkler U.** 2005. Glycolate metabolism in green algae. *Physiologia Plantarum* **123**, 235–245.
- Suzuki K, Iwamoto K, Yokoyama S, Ikawa T.** 1991. Glycolate-oxidizing enzymes in algae. *Journal of Phycology* **27**, 492–498.
- Tolbert NE.** 1997. The C₂ oxidative photosynthetic carbon cycle. *Annual Review of Plant Physiology and Plant Molecular Biology* **48**, 1–25.
- Wagner C, Sefkow M, Kopka J.** 2003. Construction and application of a mass spectral and retention time index database generated from plant GC/EI-TOF-MS metabolite profiles. *Phytochemistry* **62**, 887–900.
- Wingler A, Lea PJ, Leegood RC.** 1999. Photorespiratory metabolism of glyoxylate and formate in glycine-accumulating mutants of barley and *Amaranthus edulis*. *Planta* **207**, 518–526.
- Wingler A, Lea PJ, Quick WP, Leegood RC.** 2000. Photorespiration: metabolic pathways and their role in stress protection. *Philosophical Transactions of the Royal Society B: Biological Sciences* **355**, 1517–1529.
- Yamaguchi K, Nishimura M.** 2000. Reduction to below threshold levels of glycolate oxidase activities in transgenic tobacco enhances photoinhibition during irradiation. *Plant Cell Physiology* **41**, 1397–1406.
- Zelitch I.** 1972. The photooxidation of glyoxylate by envelope-free spinach chloroplasts and its relation to photorespiration. *Archives of Biochemistry and Biophysics* **150**, 698–707.